



HEMATOLOGY, TRANSFUSION AND CELL THERAPY

www.htct.com.br


Original article

Hypoxic conditions confer chemoresistance to crizotinib but not to imatinib in chronic myeloid leukemia cells

Q1 Lena Avinery ^{a,1}, Danielle Regev ^{b,1}, Hazem Khamaisi ^a, Jacob Gopas ^b, Jamal Mahajna ^{a,*}

^a Department of Nutrition and Natural Products, Migal Galilee Research Institute, Kiryat Shmona, and department of Biotechnology, Tel-Hai College, Kiryat Shmona, Israel

^b Shraga Segal Department of Microbiology, Immunology and Genetics, Ben Gurion University of the Negev, Beer Sheva, Israel

Q2

ARTICLE INFO

Article history:

Received 23 February 2025

Accepted 24 August 2025

Available online xxx

Keywords:

Hypoxia

Chronic myeloid leukemia

Bcr/abl

Chemoresistance

Imatinib

Crizotinib

2-methoxyestradiol

ABSTRACT

Introduction: Chronic myeloid leukemia is an adult leukemia, constituting 15 % of all leukemia diagnoses. The fundamental driver of disease pathogenesis is the Bcr/Abl fusion protein, characterized by dysregulated tyrosine kinase activity. Abl kinase inhibitors have become the mainstay of treatment, however, patients often develop resistance due to genetic alterations, particularly affecting the Bcr/Abl oncoprotein. The tumor microenvironment is also associated with acquired resistance to Abl kinase inhibitors in chronic myeloid leukemia.

Methods: The influence of hypoxic conditions on the development of chemoresistance to certain Abl kinase inhibitors was investigated in chronic myeloid leukemia.

Results: This study showed that hypoxia increased resistance to crizotinib, while imatinib resistance was modest. Both drugs effectively inhibited Bcr/Abl activity. Interestingly, the JAK1/2 inhibitor ruxolitinib further enhanced chemoresistance to crizotinib under hypoxic conditions. Hypoxia-inducible factor 1 α (HIF1 α) overexpression in JAK2 knockdown experiments confirmed their cooperative role in mediating crizotinib resistance. In addition, 2-methoxyestradiol, a non-estrogenic estradiol metabolite, restored crizotinib sensitivity under hypoxia and the combination of 2-methoxyestradiol with a JAK2 inhibitor showed promising results in overcoming crizotinib resistance.

Conclusion: In summary, this study shows the critical role of selective targeting of components of the HIF1 α signaling pathway for the complete eradication of chronic myeloid leukemia cells.

© 2025 Published by Elsevier España, S.L.U. on behalf of Associação Brasileira de Hematologia, Hemoterapia e Terapia Celular. This is an open access article under the CC BY license (<http://creativecommons.org/licenses/by/4.0/>).

Introduction

Q3

Philadelphia chromosome-positive (pH⁺) leukemia is defined by the chromosomal translocation t(9;22), which leads to the

3

* Corresponding author.

E-mail address: jamalm@migal.org.il (J. Mahajna).

¹ LA and DR equally contributed to this work

<https://doi.org/10.1016/j.htct.2025.106240>

2531-1379/© 2025 Published by Elsevier España, S.L.U. on behalf of Associação Brasileira de Hematologia, Hemoterapia e Terapia Celular. This is an open access article under the CC BY license (<http://creativecommons.org/licenses/by/4.0/>).

4 formation of the *Breakpoint Cluster Region/Abelson proto-onco-*
5 *gene 1* fusion gene (*Bcr/Abl*). Persistent activation of *Bcr/Abl*
6 leads to increased cell proliferation, decreased sensitivity to
7 various apoptotic signals, and neoplastic transformation [1].
8 Abl kinase inhibitors (AKIs) are used to treat pH^+ leukemia.
9 Although these treatments are initially effective [2], their clin-
10 ical efficacy declines with disease progression. Patients with
11 chronic myeloid leukemia (CML) in blast crisis or acute lym-
12 phoblastic leukemia (pH^+) rarely, if ever, benefit from AKI
13 therapy [3]. *Bcr/Abl*-dependent or independent mechanisms
14 may be responsible for resistance to therapy in pH^+ leukemia.
15 A significant contributing factor to drug resistance in pH^+ leu-
16 kemia is the bone marrow (BM) niche, which is a part of the
17 tumor microenvironment (TME). The BM microenvironment
18 is crucial for controlling stem cells and long-term hematopoi-
19 esis [4]. Nonetheless, soluble growth factors, interleukins,
20 stromal cells, and extracellular components—all of which are
21 found in the BM niche—may help reduce the susceptibility of
22 cancer cells to treatment [5]. To overcome treatment failure
23 in pH^+ leukemia, new therapeutic approaches must be devel-
24 oped considering these drug resistance mechanisms medi-
25 ated by the BM microenvironment.

26 The BM microenvironment can consist of areas of hypoxia
27 (low oxygen) and acidity, which can interfere with the ability
28 of chemotherapy to effectively treat tumor cells. Furthermore,
29 hypoxia in the microenvironment has been associated with
30 metastasis, malignant invasion, and a cellular transformation
31 known as the epithelial-mesenchymal transition (EMT).

32 Both malignant and normal hematopoietic stem cells,
33 including those from CML, may encounter a hypoxic niche in
34 the BM microenvironment. High BM hypoxia levels have been
35 linked to resistance to therapies in several malignancies [6],
36 minimal residual disease persistence [7], and disease progres-
37 sion. A major factor in the course of the disease is the interac-
38 tion between leukemic cells and their surroundings.

39 The interaction of leukemic cells with their environment
40 plays a significant role in the progression of the disease. HIF-
41 1α , an important regulator of the cellular response to low oxy-
42 gen, is necessary for metabolic adaptability and proliferation
43 under hypoxic conditions. HIF- 1α stabilizes in hypoxic condi-
44 tions and suppresses programmed cell death (apoptosis) by
45 either directly or indirectly controlling the expression of sev-
46 eral genes that mediate chemoresistance. The genes which
47 have been shown to be regulated by HIF- 1α include *Bak*, *Bax*,
48 *Bcl-xL*, *Bcl-2*, *Bid*, *Mcl-1*, *NF- κ B*, and *p53* [8]. Notably, whereas
49 HIF- 1α activation of anti-apoptotic target genes is well-estab-
50 lished, the exact biological mechanisms underlying this phe-
51 nomenon are still only partially known [9]. New data further
52 emphasizes how the microenvironment mediates resistance
53 to several Abl kinase inhibitors, including imatinib, nilotinib,
54 and Dasatinib [10]. Furthermore, the microenvironment has
55 been linked to the persistence of residual diseases of pH^+ leu-
56 kemia [11].

57 Even though imatinib actively inhibits *Bcr/Abl* kinase, pH^+
58 leukemia cells under hypoxic conditions show partial sup-
59 pression of apoptosis [12]. Given that BM microenvironment
60 cells secrete soluble molecules including SDF-1, vascular
61 endothelial growth factor (VEGF), and interleukin-6, which
62 are all known to promote the survival of hematopoietic
63 stem cells (HSCs), hypoxia may indirectly contribute to

chemoresistance [13]. Chemotherapy resistance mediated by 64
the BM microenvironment is still a major challenge in the 65
treatment of leukemia. 66

The present study investigated how hypoxia affects the 67
efficacy of the tyrosine kinase inhibitor crizotinib by exploring 68
its off-target activities, rather than its established function as 69
an anaplastic lymphoma kinase (ALK) inhibitor implicated in 70
ALK-positive non-small cell lung cancer (NSCLC). This study 71
aims to repurpose crizotinib for an additional therapeutic 72
indication—specifically, to overcome chemoresistance in 73
CML which is the focus of our research program. 74

Materials and methods 75

Chemicals and reagents 76

Sigma Aldrich Israel Ltd. (Rehovot, Israel) provided most of 77
the chemicals, including cobalt chloride (CoCl_2). The text 78
includes specific sources for various compounds. 2-Methox- 79
yestradiol (2ME2) was purchased from Cayman Chemical 80
(Ann Arbor, MI, USA), Everolimus (Afinitor) and kinase inhibi- 81
tors (Imatinib, Ruxolitinib, and Crizotinib) were obtained from 82
Selleck Chemicals LLC (Houston, TX, USA). 83

Cell lines 84

The American Type Culture Collection (ATCC, VA, USA) pro- 85
vided the human CML cell lines K562 and BV173. The cells 86
were cultured in complete RPMI 1640 media supplemented 87
with 0.1 mg/mL streptomycin, 100 units/mL penicillin, 1 % (w/ 88
v) L-glutamine, and 10 % (w/v) fetal bovine serum (Biological 89
Industries, Israel). All cells were maintained in a humidified 90
incubator with 5 % CO_2 at 37 °C. 91

HIF1 α overexpression 92

Using a retrovirus harboring HA-HIF1 α P402A/P564A (Addgene 93
plasmid #1900 [14]), K562 cells were stably transfected to over- 94
express HIF1 α , as previously reported [15]. In summary, puro- 95
mycin selection was used to isolate stable transfected cells 96
after K562 cells were infected with the retrovirus. Overexpres- 97
sion of HA-HIF1 α was detected in the transfected cells using 98
immunoblotting with anti-HIF1 α antibodies. 99

JAK2 silencing in K562 cells 100

Using a previously established CRISPR-Cas9 method, JAK2 101
expression was suppressed in K562 cells [15]. In summary, 102
lenti-cas9blast (Addgene plasmid #52,962), gRNA JAK2 (Add- 103
gene plasmid #75,728), and lentiviral packaging plasmids 104
(pcMV-dR8.2 dvpr and pcMV-VSV-G) (Addgene plasmids 105
#8455 and #8454) [16] were co-transfected into HEK293T cells 106
(1.5×10^5 cells/mL) using Eugene 6 transfection reagent 107
(Roche Applied Science, Penzberg, Germany) according with 108
the manufacturer's instructions. The supernatant containing 109
the lentiviral particles was collected 48 h post-transfection 110
and utilized to infect K562 cells. Then, stably transduced 111
clones with decreased JAK2 expression were isolated using 112
blasticidin and puromycin selection. Western blotting was 113

performed to confirm the downregulation of JAK2 protein levels.

Cell viability assay

The trypan blue exclusion assay was used to assess cell viability. K562 cells were seeded at a density of 2×10^5 cells per well in six-well plates. Cells were subjected to the specified treatments following a 24-hour incubation period. Dimethyl sulfoxide (DMSO) at a concentration of 1% (w/v) was applied to the control samples. After exposure for 72 h, cells were collected, stained with a 0.4% (w/v) trypan blue solution diluted 1:1 with culture media, and then manually counted using a hemocytometer according to the previous described protocol.

Western blotting

Phosphatase inhibitors (AG Scientific, CA, USA) were used to produce cell lysates. After lysing the cell pellets in the buffer for half an hour on ice, the supernatants were separated by centrifugation. The DCTM Protein Assay (Bio Rad, USA) was used to determine the protein concentration in the supernatants (absorbance measured at 630 nm). Equal protein concentrations (50–60 µg each sample) were electrophoretically separated after being loaded onto 8–12% polyacrylamide gels. After that, the proteins were transferred onto nitrocellulose membranes (Schleicher & Schuell BioScience GmbH, Germany). To decrease non-specific antibody binding, the membranes were then blocked using 5% non-fat dried milk in Tris-buffered saline with Tween 20 (TBS-T).

To detect the presence of phospho-Abl (Tyr 245) and cleaved PARP (Poly(ADP-ribose) Polymerases - Cell Signaling Technology, MA, USA), α -tubulin (Santa Cruz Biotechnology, TX, USA), and phospho-ERK1/2 (Thr202/Tyr204) (Cell Signaling Technology, MA, USA), primary antibodies were employed. Every primary antibody incubation was carried out following the instructions recommended by the manufacturer.

Species-specific secondary antibodies combined with horseradish peroxidase (HRP), such as anti-mouse (NB7539, Novus Biologicals, CO, USA) and anti-rabbit (#7074, Cell Signaling Technology), were used to detect the bound primary antibodies. The SuperSignalTM West Pico PLUS chemiluminescent substrate (Thermo Fisher Scientific, MA, USA) was used following the manufacturer's instructions to accomplish chemiluminescent detection [17,18].

Flow cytometry analysis

The expressions of CD45 and CD44 on the cell surface were evaluated by flow cytometry, as previously reported [15]. In short, K562 cells were resuspended at a density of 1×10^7 cells/mL in phosphate-buffered saline (PBS) containing 0.5% bovine serum albumin (BSA), together with K562/HIF1 α and K562/Si JAK2 variations. The CD45 (KRO, #A96416, Beckman Coulter) and CD44 antibodies (FITC, #9011–0441, eBioscience) were either employed at the dilutions suggested by the manufacturer or titrated in advance to maximize staining. For forty minutes, the cell-antibody combination was incubated on ice. The labeled cells were analyzed using a Beckman Coulter

Navios flow cytometer after washing with PBS mixed with 0.5% BSA.

RNA extraction and cDNA synthesis

Using Tri Reagent (Sigma), total RNA was isolated from cells following a previously described procedure [15]. The isolated RNA was then subjected to reverse transcription (RT), which produced single-stranded cDNA. In short, 15 µL of nuclease-free water (DEPC-treated) and 1 µL of oligo(dT)17 primer were added to 1 µg of RNA, and the mixture was pre-incubated for 10 min at 70 °C before being quickly cooled on ice. Second, 2 mL of 5X AMV RT reaction buffer, 2 µL of dNTP mix (25 mM), 28 units of RNasin ribonuclease inhibitor, 30 units of AMV reverse transcriptase, and nuclease-free water were added to the annealed primer-template mixture for a final volume of 10 µL. The RT reaction was incubated for 60 min at 42 °C.

Polymerase chain reaction (PCR) amplification

A commercial PCR kit (Bioline, Taunton, MA, USA) was used to amplify the generated cDNA. Specific primers for each gene of interest are specified in Table 1. Thirty-five amplification cycles (each cycle: 94 °C denaturation for 30 s, 55–60 °C annealing for 30 s, and 72 °C extension for 2 min and 30 s) proceeded after the first denaturation step at 94 °C for two minutes. The cycling program concluded with a last extension step that lasted 15 min at 72 °C. Primers specific to the housekeeping gene β -actin were used as a control. The PCR products (5 µL) were separated by electrophoresis in a 1.5% agarose gel.

Quantitative real-time polymerase chain reaction (RT-PCR)

Quantitative RT-PCR amplification of mRNA transcripts was performed using the resultant cDNA. Each 15 µL reaction mixture included 1X SYBR GREEN reaction mix (Kappa Biosystems, Wilmington, MA, USA) and 0.2 pmol/µL of forward and reverse primers. A spectrofluorometric Rotor-Gene 6000 thermal cycler (Corbett Research, Mortlake, Australia) was used to perform the PCR. The Taq DNA polymerase was first activated by a 10-minute denaturation stage at 95 °C, which was followed by 55 cycles of denaturation at 95 °C for 15 s and a one-minute combined annealing/extension step at 55–60 °C. A range of cDNA template concentrations were evaluated to guarantee amplification within the linear range. As an

Table 1 – Oligonucleotide primers for gene amplification.

Primers	Forward	Reverse
hVEGF	5'-GTCGGGCGCTCCGAAAC-CATG-3'	5'-CCTGGTGAGA-GATCTGGTTC-3'
hBcl2	5'-CTGGAGAGTGCTGAA-GATTGATG-3'	5'-CAATCACGCGGAA-CACCTTGATTC-3'
hMcl1	5'-GATCAGTATATACACTT-CAG-3'	5'-CAGGTGCAGCCTG-TACTTGTC-3'
h β -actin	5'-GCCCTGGACTTCGAG-CAAGA-3'	5'-TGCCAGGGTA-CATGGTGGTG-3'

Sequences of the forward and reverse primers used for polymerase chain reaction along with their corresponding target genes.

internal control, the housekeeping gene β -actin was co-amplified in the same PCR reaction. The primer sequences employed in the semi-quantitative RT-PCR were the same.

Colony formation assay

A clonogenic experiment was used to evaluate the capacity of cells to form colonies on a semi-solid medium, as previously reported [19]. In summary, K562 cells were diluted in complete RPMI 1640 media with 10 % fetal bovine serum (FBS) until they reached a density of 1×10^4 cells/mL. The cell suspension was mixed with an equivalent amount of 0.6 % agar solution to reach a final agar concentration of 0.3 %. The cell-agar mixture was plated in 12-well plates over a layer of bottom agar that had already hardened and left to solidify. To maintain agar hydration after the top layer solidified, 1 mL of new medium containing the specified treatments was applied to each well. The cells were cultured for two weeks at 37 °C in a humidified environment with 5 % CO₂ to enable colony formation. A colorimetric MTT (3-(4,5-dimethylthiazol-2-yl)-2,5-diphenyltetrazolium bromide) test was used to visualize and quantify colonies. The plates were incubated for 4 h with 5 mg/mL MTT solution, followed by the extraction of the formazan product using a solubilization buffer (20 % SDS, 50 % N,N-dimethylformamide, and 25 mM HCl). Using a plate reader, the optical density of the extracted dye was measured with a plate reader at 570 nm with a reference wavelength of 630 nm.

Hypoxic conditions

A hypoxic atmosphere was created using a BioSpherix OxyCycler system (BioSpherix, Redfield, NY, USA). Cells were cultured in a custom-designed, computer-controlled incubator attached to the OxyCycler. A controlled environment of 37 °C, 5 % CO₂, and 2 % O₂ was maintained in the hypoxic chamber. The cells in the control group were cultured for the duration of the experiment in normoxic conditions (~21 % O₂ and 5 % CO₂). Twelve hours was the incubation time for both normoxic and hypoxic experiments.

Immunofluorescence staining and imaging

The cellular expression and location of phospho-c-Abl and HIF-1 α proteins in K562 cells were determined by immunofluorescence. The immunofluorescence protocol involved coating a 96-well plate with poly-L-lysine (Sigma Aldrich Israel Ltd, Rehovot, Israel) four hours before the experiment completion and allowing it to dry for two hours. Following the seeding of 5×10^5 cells in the coated wells, they were incubated for a further two hours under normoxic conditions and then 12 h of normoxic/hypoxic conditions as described above.

Following incubation, cells were washed twice with PBS and fixed with 4 % paraformaldehyde in PBS for 20 min at room temperature (RT). Following fixation, cells were washed twice with PBS and permeabilized using a solution containing 3 % FBS and 0.1 % Triton X-100 in PBS for 1 h at room temperature. Blocking was carried out for an extra one hour at room temperature using the same permeabilization solution. The primary antibody of interest (HIF1 α or phospho-c-Abl) was then diluted in 3 % FBS and 0.1 % Triton X-100 in PBS. Cells

were incubated overnight after being thoroughly washed twice with 3 % FBS in PBS. DAPI (nuclear stain) and Alexa Fluor-688 (red) (Thermo Fisher Scientific, Waltham, MA, USA), a secondary antibody, were added to the cells and incubated for 30 min the next day. The last washing step was three washes using 0.1 % Triton X-100 in 3 % FBS and PBS.

Image Acquisition used a 20x magnification with images being taken with the Zeiss Cell Discoverer 7 Imaging System. The picture capture program was Zen Blue 3.7.

Protein Expression Quantification: Immunofluorescence data were used to quantify the relative amounts of phospho-c-Abl and HIF-1 α protein expression.

Statistical analysis

Data were analyzed using Student's t-test. Statistical significance was set at a *p-value < 0.01 and **p-value < 0.001.

Results

A previous study showed that Crizotinib, an ALK and c-Met inhibitor is able to inhibit both wild-type and T315I-mutated Bcr/Abl [20]. In addition, another study reported that Crizotinib, but not Imatinib, was able to overcome soluble factor-mediated drug resistance in CML cells [21]. This was possible in part because Crizotinib could inhibit JAK2 activity. In the present study, normoxic and hypoxic conditions were used to evaluate the sensitivity of CML cell lines to Abl kinase inhibitors such as Imatinib and Crizotinib.

Induction of apoptosis in chronic myeloid leukemia cells by imatinib and crizotinib under hypoxic conditions

CoCl₂, a known inducer of HIF1, was used to simulate hypoxic conditions in the K562 and BV173 CML cell lines [22]. Immunofluorescence analysis showed that K562 cells exposed to 100 μ M CoCl₂ exhibited increased levels of HIF1 comparable to exposure to low oxygen (Figure 1A and B). Real-time PCR was also used to monitor the expression of HIF1-responsive genes such as VEGF and Bcl2 (Figure 1C) and to demonstrate the functionality of induced HIF1 in K562 cells treated with CoCl₂.

Exposure to CoCl₂ and growth of K562 under hypoxic conditions led to an accumulation of HIF1 α (Figure 1A and B), which increased the expression of VEGF and Bcl2 by more than fourfold and twentyfold, respectively (Figure 1C). Figure 1D shows that CoCl₂ treatment had no effect on Abl phosphorylation in K562. The study also showed that Imatinib and Crizotinib alone or in combination with Ruxolitinib inhibited the phosphorylation of Abl under normoxic (Figure 1D and E) and hypoxic (Figure 1F and G) conditions. Interestingly, pAbl levels were lower in hypoxic conditions (Figure 1E) compared to normoxic conditions (Figure 1G).

Next, how Imatinib and Crizotinib affected the proliferation of K562 cells in the presence and absence of CoCl₂ was examined. Figure 2A shows that exposure to imatinib inhibited the proliferation of K562 in the presence or absence of CoCl₂. In addition, a significant inhibition of cell proliferation in K562 cells treated with Crizotinib was observed. However,

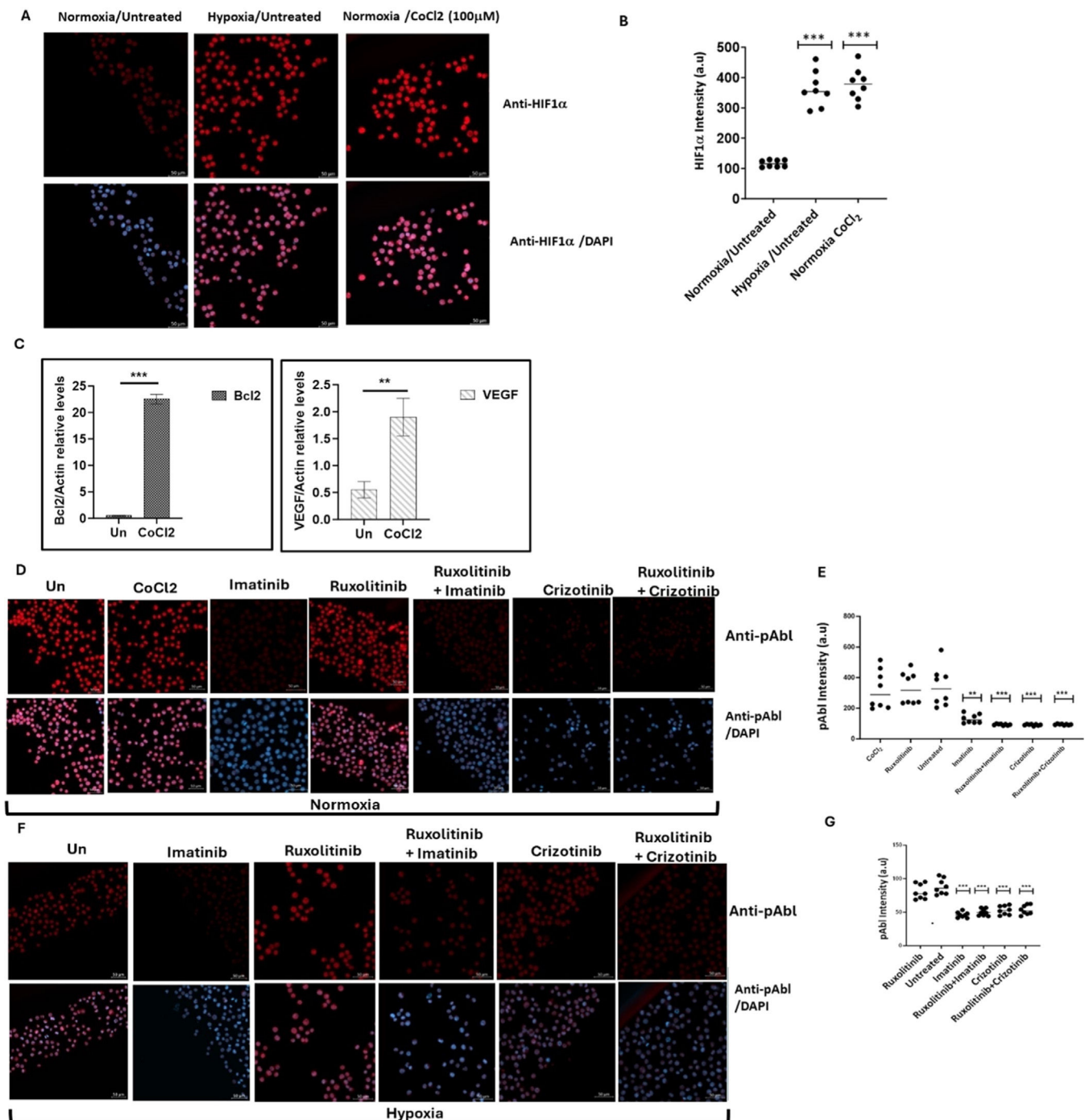


Figure 1 – Expression of HIF1α and pAbl in K562 under hypoxic conditions. K562 cells were treated with 100 μM cobalt chloride (CoCl₂) or grown under low oxygen conditions (2 %) for 12 h. (A) Induction of HIF1α in K562 cells by treatment with CoCl₂ and exposure to hypoxic conditions for 12 h. (B) Quantitation of HIF1α levels under the different conditions. (C) Real-time PCR was used to determine the relative expression of Bcl2 and VEGF in relation to β-actin in K562 cells exposed to 100 μM CoCl₂. Sequences of the primers used in this study are shown in Table 1. (D) Immunofluorescence assessment of pAbl levels in K562 cells grown under normoxic, and (E) quantitation. (F) Immunofluorescence assessment of pAbl levels in K562 cells grown under hypoxic conditions after 12 h of treatment, Imatinib, Ruxolitinib, Imatinib/Ruxolitinib, and Crizotinib/Ruxolitinib and (G) quantitation. *p-value ≤ 0.01, **p-value ≤ 0.001, *** p-value ≤ 0.0001. The experiment, performed in duplicate, was repeated, with consistent results observed across both independent experiments.

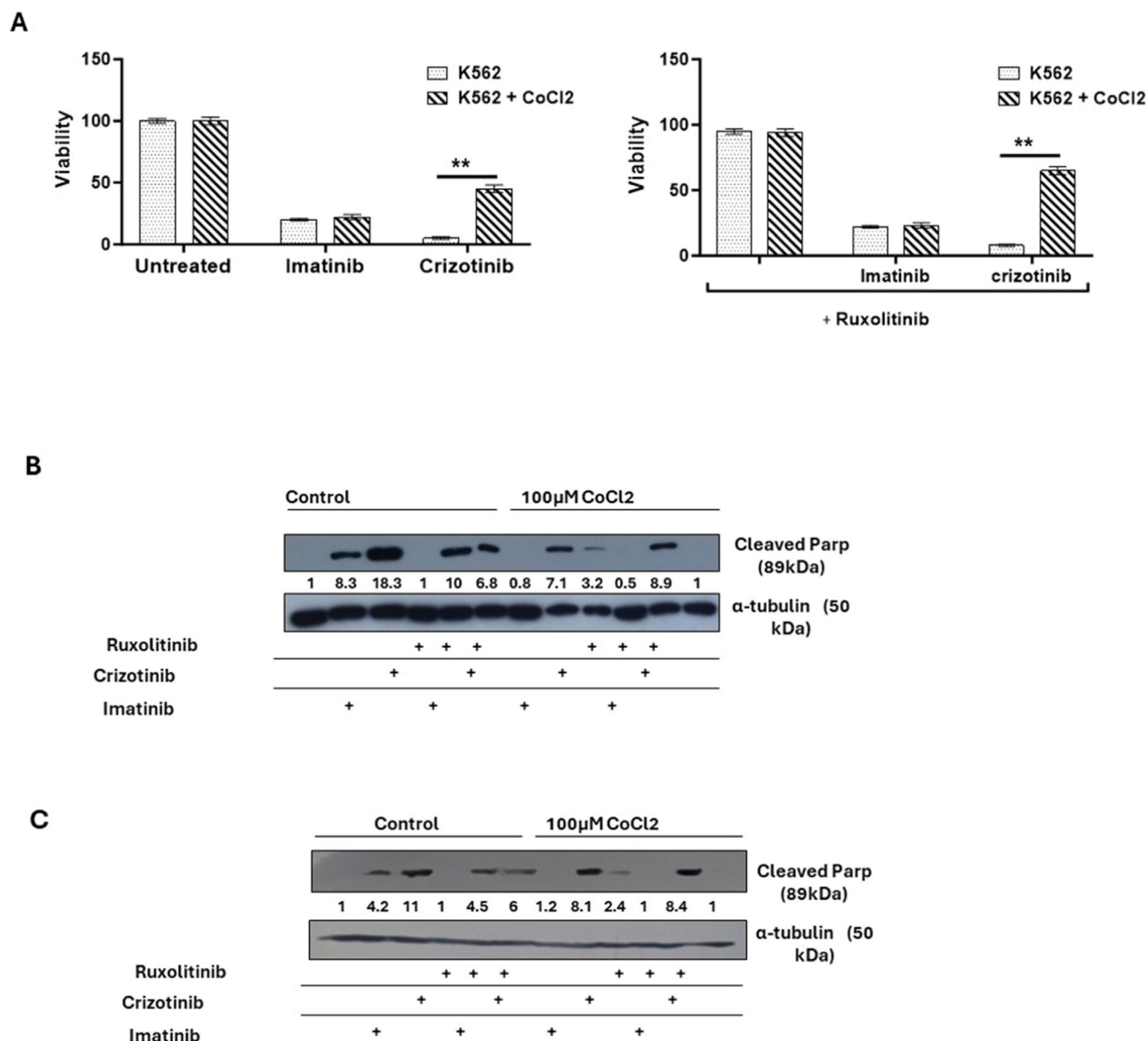


Figure 2 – Effect of cobalt chloride (CoCl₂) and ruxolitinib on the sensitivity of K562 and BV 173 cells to treatment with Imatinib or Crizotinib. K562 or BV 173 cells exposed to 100 μM CoCl₂ and treated with 1 % DMSO, 1 μM Imatinib, Crizotinib or Ruxolitinib for 12 h. (A) Measurement of the viability of K562 with the trypan blue exclusion assay using a two-sample t-test. Immunoblot of (B) K562 and (C) BV 173 cells exposed to 1 μM Imatinib, Crizotinib, and Ruxolitinib in the presence or absence of 100 μM CoCl₂. Filters were probed with anti-c-PARP and α-tubulin antibodies. The numbers below the plot represent the relative expression levels normalized to α-tubulin.

moderate drug resistance was observed in the presence of CoCl₂ in Crizotinib-treated K562 cells. This suggests that the presence of CoCl₂ blocks the inhibition of cell proliferation mediated by Crizotinib but not by Imatinib (Figure 2A). Signal Transducer and Activator of Transcription 3 (STAT3) has been associated with hypoxia-induced chemoresistance of ovarian cancer cells [23]. Therefore, the JAK1/2 inhibitor Ruxolitinib [24], which regulates the activity of STAT3, was used to investigate the role of JAK1/2 in the sensitivity of CML cells to

Crizotinib. We wondered whether the addition of Ruxolitinib to Crizotinib in the presence of CoCl₂ could restore sensitivity. Treatment with Ruxolitinib alone had no effect on the proliferation of K562 cells in the presence or absence of CoCl₂ (Figure 2B). Furthermore, there was no significant difference in the inhibition of K562 cell proliferation between the combinations of Imatinib and Ruxolitinib (Figure 2B). Interestingly, the combination of Ruxolitinib and Crizotinib did not restore the sensitivity of K562 to Crizotinib. In contrast, the inclusion

of Ruxolitinib increased Crizotinib resistance in K562 cells (Figure 2B). Comparable data were also obtained using other CML cells such as BV173 (Figure 2C).

The role of HIF1 α and JAK2 in mediating chemoresistance in chronic myeloid leukemia

The above data suggests that the sensitivity of CML cells to Crizotinib is dependent on JAK1/2 activity and hypoxic conditions (Figure 2). However, neither hypoxia nor JAK1/2 activity had a significant effect on sensitivity to Imatinib (Figure 2). HIF1 α is an important mediator of hypoxic conditions and modulates the transcription of many genes. To directly demonstrate the role of hypoxia and JAK2 in regulating sensitivity to Crizotinib, a stable mutant of HIF1 α (Pro 402 and Pro 564 were replaced by Ala) [25] was overexpressed in K562. Under normoxic conditions, the HIF1 α mutant Pro 402 Ala, Pro 564 Ala is not hydroxylated and is therefore not recognized by the von Hippel-Lindau tumor suppressor protein (VHL) for proteasome degradation [26]. Figure 3A shows that HA-HIF1 α is overexpressed in K562/HIF1 cells under normoxic conditions. CD44 is one of the genes regulated by HIF1 α [27], and monitoring of levels in K562 and K562/HIF1 α cells showed upregulation of CD44 (Figure 3B).

Next, the activity of the Abl inhibitor in K562 cells stably expressing HIF1 α was examined. The levels of phosphorylated Bcr/Abl and Abl were essentially unaffected by the overexpression of HIF1 α , as shown in Figure 3C. However, the levels of phosphorylated Bcr/Abl and Abl in K562 and K562/HIF1 α lysates were completely inhibited by Imatinib or Crizotinib alone or in combination with Ruxolitinib (Figure 3C). This suggests that the ability of Imatinib and Crizotinib to inhibit auto-phosphorylation of the Abl protein is not affected in cells overexpressing HIF1 α or exposed to Ruxolitinib. When K562 cells were exposed to Imatinib, PARP was significantly cleaved. Interestingly, the combination of Ruxolitinib and Imatinib decreased the amount of cleaved PARP in K562/HIF1 α cells but not in K562 cells. The amount of cleaved PARP was almost twice as high in Crizotinib-treated K562 cells compared to Imatinib-treated cells. In addition, the combination of Ruxolitinib and Crizotinib significantly reduced the amount of cleaved PARP in K562 by about 50 %. In contrast, neither Crizotinib nor Crizotinib in combination with Ruxolitinib resulted in cleavage of PARP in K562/HIF1 α cells. Figure 3 shows that HIF1 α is responsible for the reduction of cleaved PARP levels in K562 cells when exposed to Crizotinib, although Crizotinib still inhibits Bcr/Abl activity. In addition, it supports the notion that JAK1/2 inhibition contributes to the reduced sensitivity of Imatinib and Crizotinib.

A comparison of the effect of Imatinib and Crizotinib was also evaluated using a clonogenicity assay. Figure 3D shows that Imatinib inhibited colony formation in K562 and K562/HIF1 α cells at concentrations of 1 and 3 μ M. Crizotinib was more effective in inhibiting colony formation of K562, and significant inhibition was observed at the lowest concentration (0.3 μ M). The ability of Crizotinib to inhibit K562/HIF1 α was impaired, indicating some degree of resistance. Interestingly, the addition of Ruxolitinib reduced the ability of Crizotinib to inhibit colony formation in both K562/HIF1-positive and -negative cells. Of note, the combination of Ruxolitinib with

Crizotinib showed a minimal effect on the proliferation of K562 (Figure 2A - cells grown in two-dimensional [2D] culture) and a significant effect on K562 treated with Crizotinib plus Ruxolitinib in a three-dimensional (3D) culture (Figure 3D).

The JAK2 gene was also silenced in K562 cells (Figure 4A). The sensitivity of K562, K562/Si JAK2 and K562/ HA-HIF1 α P402A/P564A to a range of Abl kinase inhibitors (AKIs) was monitored. The results shown in Figure 4B demonstrate that the different cells have different sensitivities to the different AKIs.

Exposure of various K562 cells to AKIs resulted in a decrease in cell viability. When K562/HIF1 α cells were treated with AKIs, a marked and reproducible increase in cell viability was observed compared to K562 cells (Figure 4B), indicating partial drug resistance due to overexpression of HIF1 α (Figure 4B). The ability of Crizotinib to inhibit the proliferation of K562 cells was significantly different from that of K562/Si JAK2 and K562/HIF1 α cells. Crizotinib was less effective in inhibiting the proliferation of K562/Si JAK2 and K562/HIF1 α cells (Figure 4B). Thus, the percentages of viable cells in K562, K562/Si JAK2, and K562/ HA-HIF1 α when exposed to 500 nM Crizotinib for 72 h were 23.4, 57.9, and 63.4, respectively (Figure 4C). In addition, no significant differences in cell viability were observed between K562 cells exposed to other AKIs, including ponatinib and GNF-5 (Figure 4B). These results suggest that the reduced sensitivity to Crizotinib is significant in cells overexpressing HIF1 α or silenced with JAK2, whereas it is less evident with other AKIs.

2-methoxyestradiol restores crizotinib sensitivity of CML cells under hypoxic conditions

The data of this study suggest that HIF1 α is responsible for mediating Crizotinib chemoresistance in CML cells. Therefore, it investigated whether HIF1 α modulators can restore sensitivity to Crizotinib. Two HIF1 α modulators, 2ME2 and Everolimus (Afinitor), were used. 2ME2, a natural estradiol metabolite, has been shown to inhibit the nuclear accumulation and activity of HIF1 α in an oxygen- and proteasome-independent manner [28], while Afinitor, an mTOR inhibitor, has been shown to reduce the expression of HIF1 α and restore chemosensitivity in ALL cells [29].

Figure 5A shows that Crizotinib induces PARP cleavage in K562 cells but not in K562/HIF1 α cells. However, 2ME2 was only marginally active in inducing PARP cleavage in K562 cells, whereas Afinitor was not. The combination of Afinitor with Crizotinib had little effect on the sensitivity of K562 cells to Crizotinib, particularly in K562/HIF1 α cells. In contrast, the combination of 2ME2 and Crizotinib significantly increased the amount of cleaved PARP in K562/HIF1 α cells, suggesting that 2ME2 can restore the sensitivity of Crizotinib in K562 cells overexpressing activated HIF1 α . Thus, the decreased sensitivity of CML cells to Crizotinib under hypoxic conditions is primarily mediated by the stabilization and increased activity of HIF1 α , and inhibiting the function of HIF1 α may restore the sensitivity of Crizotinib in hypoxic CML cells.

To explore the possible mechanism by which activation of HIF1 α confers chemoresistance to CML cells despite complete inhibition of Bcr/Abl, changes in apoptosis-related gene expression were monitored in K562 and K562/HIF1 α cells

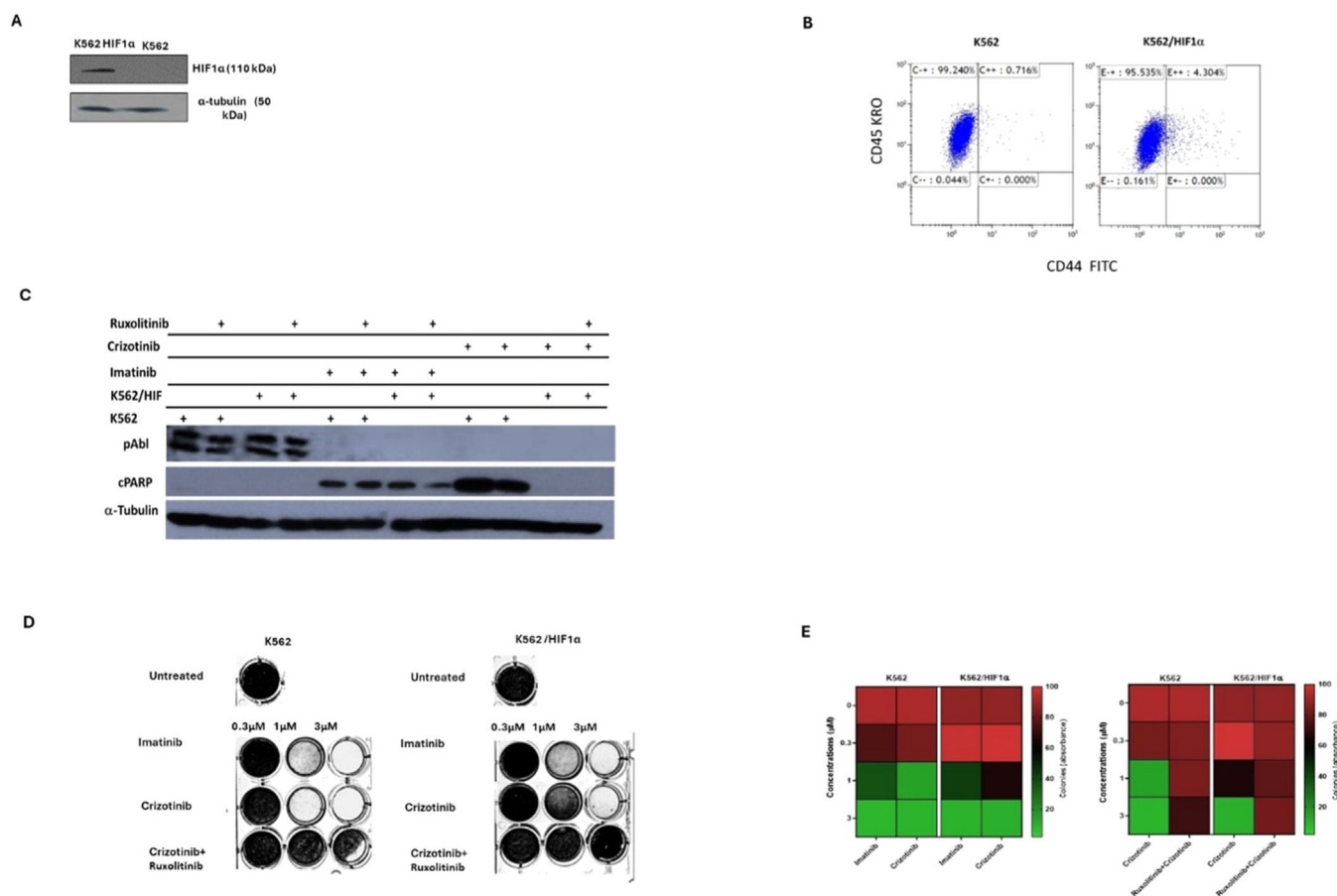


Figure 3 – Effect of overexpression of HIF1α on the chemoresistance of K562. (A) Immunoblot of HIF1α in K562 and K562/HIF1α cells. (B) The level of expression of CD44 in K562 and K562/HIF1α was determined by FACS analysis. (C) Levels of pAbl and cleaved PARP in K562 and K562/HIF1α exposed to Imatinib (1 μM), Crizotinib (1 μM), or Ruxolitinib (1 μM) for 24 h. (D) Clonogenicity of K562 and K562/HIF1α cells under semi-solid conditions in the presence of Imatinib (0.3, 1 and 3 μM) and Crizotinib (0.3, 1 and 3 μM) in combination with Ruxolitinib (1 μM). (E) Heatmap of absorbance of dye levels extracted from stained colonies in the different samples. The experiment was performed twice, yielding comparable results.

448 treated with Crizotinib. The expression of *Mcl1* and *Bcl2* genes
 449 in K562 and k562/HIF1α cells treated with Imatinib or Crizoti-
 450 nib were monitored (Figure 5B). Treatment of K562 cells with
 451 Imatinib resulted in a small reduction in the levels of both
 452 genes. Treatment with Crizotinib was more effective in reduc-
 453 ing the levels of the *MCL1* and *Bcl2* genes. In contrast, treat-
 454 ment with Imatinib in K562/HIF1α led to a similar reduction
 455 in the levels of both genes as in K562 cells. However, the levels
 456 of *Bcl2* and *MCL1* were significantly higher in Crizotinib-
 457 treated K562/HIF1α cells than in Imatinib-treated cells. This
 458 suggests that the levels of the two anti-apoptotic genes *Bcl2*
 459 and *MCL1* are relatively higher in K562/HIF1α exposed to Cri-
 460 zotinib compared to Imatinib treatment and likely contribute
 461 to the chemoresistance to Crizotinib observed in CML cells
 462 under hypoxic conditions.

463 Discussion

464 Crizotinib inhibits native and mutant Bcr/Abl kinase activity
 465 and shows significant anti-CML activity in vitro and in vivo

[30]. In addition, Crizotinib, unlike Imatinib, can effectively
 overcome the TME-mediated chemoresistance in CML cells,
 which was attributed to the ability of Crizotinib to inhibit
 JAK2 activity [21].

This study investigated the anti-CML activity of Imatinib
 and Crizotinib under hypoxic conditions. First, it discovered
 that hypoxic conditions or exposure to CoCl₂, which mimics
 hypoxic conditions, impaired the ability of Imatinib to pro-
 mote apoptosis and inhibit proliferation (Figure 2). Neverthe-
 less, the effect of hypoxic conditions on Crizotinib-treated
 CML cells was profound and much stronger than that of Ima-
 tinib (Figure 2). The effect was not limited to inhibition of cell
 proliferation of CML, but also included the ability of treated
 CML cells to undergo apoptosis as measured by monitoring
 levels of cleaved PARP (Figure 2C and D). The observed effect
 was not limited to K562 cells, but also other myeloid cells,
 such as BV173 cells, showed a reduced ability of Crizotinib to
 induce apoptosis under hypoxic conditions compared to Ima-
 tinib-treated BV173 cells (Figure 2). The hypoxia-induced che-
 moresistance of Crizotinib in CML cells was further enhanced
 by the combination with Ruxolitinib (JAK1/2 inhibitor)

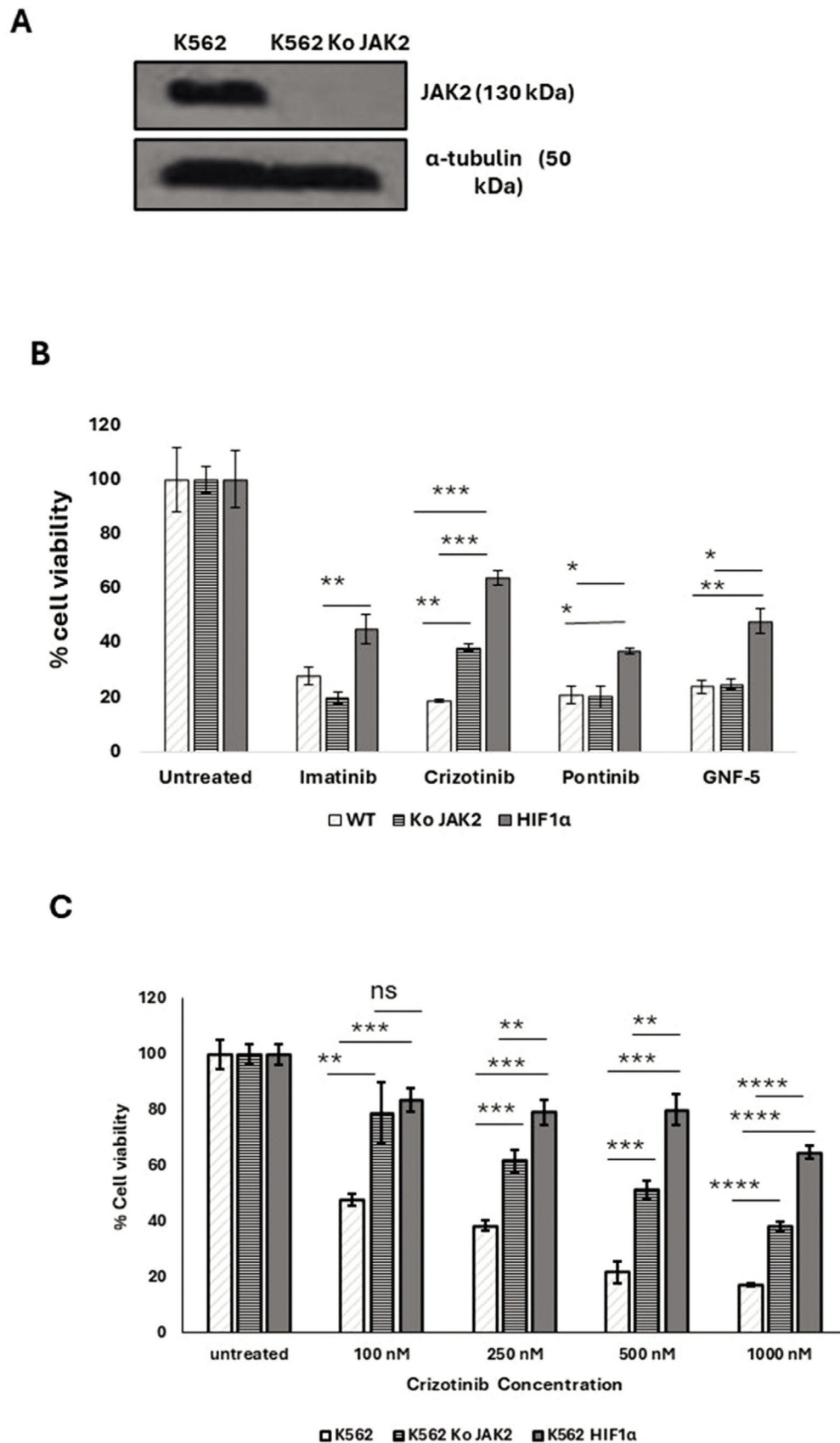


Figure 4–Effect of JAK2 silencing and HIF1α overexpression on the sensitivity of K562 to different Abl kinase inhibitor treatments. (A) Immunoblot of JAK2 in K562 and K562 SiJAK2 cells. (B) Proliferation blot showing remaining K562, K562/Si JAK2, and

(Figure 2). These results suggest that hypoxia-mediated Crizotinib resistance in CML cells is a phenomenon that is not restricted to a specific CML cell line.

Hypoxia is one of the intrinsic features of solid tumors and is associated with aggressive phenotypes such as resistance to radiotherapy and chemotherapy, metastasis, and a poor patient prognosis [31]. The BM microenvironment is a hypoxic environment that supports hematopoietic stem cells and contributes to leukemia stem cell persistence [12]. In CML, Imatinib inhibited Bcr/Abl activity in hypoxic stem cells, but apoptosis was partially inhibited [32]. Hypoxic conditions have been reported to induce resistance to Crizotinib in NSCLC cell lines with the EML4-ALK rearrangement by activating the EMT process [32]. Hypoxia could induce drug resistance via HIF1-dependent and HIF1-independent mechanisms [33,34]. To corroborate the findings of this study and provide evidence that Crizotinib-induced chemoresistance in CML cells is dependent on HIF1 α , the mutant HIF1 α was overexpressed in K562 cell lines while silencing JAK2. The mutant HIF1 α (substitution of Pro 402 and Pro 564 by Ala) [25] is not subject to hydroxylation and proteasome degradation [26] and is therefore active under normoxic conditions. K562/HIF1 α cells were almost completely resistant to Crizotinib but not to Imatinib (Figures 2 and 4), whereas K562 Si JAK2 cells were partially resistant to Crizotinib but not to Imatinib or other AKIs (Figure 4). Remarkably, the data of the current study show that Ruxolitinib, a JAK1/2 inhibitor, enhances the chemoresistance of Crizotinib under hypoxic conditions.

Of note is the ability of Ruxolitinib to enhance the chemoresistance of Crizotinib in K562 cells grown in a 3D culture (Figure 3D), whereas the effect of Ruxolitinib in a 2D culture was minimal (Figure 2A). It is well documented that cells cultured in 3D respond differently to drugs compared to cells cultured in 2D [35]. One explanation could lie in the local pH values within 2D and 3D cells, as lower pH values were found in 3D cells [36]. It is well established that lower intracellular pH values reduce the efficacy of drugs and thus contribute to drug resistance [36]. The results of this study show that the combination of Ruxolitinib with Crizotinib enhanced the chemoresistance of Crizotinib in K562/HIF1 α as well as in K562 cultured in 3D. In contrast, in a 2D culture, the effect of the combination of Ruxolitinib with Crizotinib was only observed in K562/HIF1 α cells. The data are consistent with other observations showing that cancer cell lines growing in 3D culture are more resistant to chemotherapeutic agents than in 2D culture [37].

To elucidate a possible mechanism responsible for resistance to Crizotinib under hypoxic conditions, the levels of the anti-apoptotic genes MCL-1 and Bcl2 were measured. Imatinib inhibited the expression of both anti-apoptotic genes Bcl2 and MCL1 in both cell types, although the reduction appeared to

be greater in K562/HIF1 α (Figure 5B). In contrast, Crizotinib significantly reduced the expression of Bcl2 and MCL1 in K562 cells, while increasing Bcl2 levels in K562/HIF1 α cells (Figure 5B). It is currently uncertain whether the ability of Crizotinib to upregulate Bcl2 contributes to its ability to promote chemoresistance in K562/HIF1 α cells. Hypoxic conditions inhibit the expression of pro-apoptotic genes (Bax and Bim) and stimulate the expression of anti-apoptotic genes such as Bcl-2, Mcl-1, and XIAP [38]. An alternative explanation could be related to the ability of hypoxia to induce EMT in cancer cells [39]. Exposure to Crizotinib induces EMT in NSCLC cell lines, leading to chemoresistance [32]. Therefore, one could speculate that Crizotinib treatment in the context of hypoxia may have a stronger ability to induce EMT in K562 cells than Imatinib, leading to increased chemoresistance in treated cells. This speculation still needs to be confirmed experimentally.

The known HIF1 α inhibitor 2ME2 was used to provide further evidence for the importance of HIF1 α in mediating Crizotinib chemoresistance. Figure 5 shows that 2ME2 can restore sensitivity to Crizotinib in K562/HIF1 α cells. This result is consistent with previous findings that 2ME2 can restore the sensitivity of medullary thyroid cancer (MTC) cells [40]. In addition, 2ME2 has been shown to reverse drug resistance in human breast tumor xenografts [41] and multiple myeloma cells [42]. 2ME2 is a natural metabolite of estradiol devoted to estrogenic activity. The antitumor activities of 2ME2 were mediated by its pro-apoptotic activity, microtubule activity and superoxide production [43]. In addition, 2-hydroxyestradiol, a prodrug of 2ME2, was shown to restore the sensitivity of ovarian cancer cells to platinum, which is mediated by the TME [18,44]. These results showed that the combination of 2ME2 and Crizotinib restored the sensitivity of Crizotinib in K562 cells with active HIF1 α and JAK1/2 inhibitor treatment (Figure 5). The underlying mechanism by which 2ME2 restores the sensitivity of Crizotinib is not yet clear. The main effect of 2ME2 appears to be due to disruption of the cellular microtubules required for translocation of HIF1 α to the nucleus. Thus, 2ME2 may inhibit the accumulation and activity of HIF1 α in the nucleus in a manner that is both oxygen- and proteasome-independent [28]. Consistent with previous studies, the data of the current study show that 2ME2 induces apoptosis in K562 cells [18]. Moreover, 2ME2 inhibits the proliferation of prostate cancer cells by modulating the activity of β -catenin [45]. Furthermore, 2ME2 upregulates death receptor 5 (DR5) and induces apoptosis by activating the extrinsic pathway [46]. Recent reports suggest that the antitumor activity of 2ME2 is mediated by its ability to downregulate a number of genes, including the Bcl2, BCL-XL and c-myc genes [18,47]. Overall, 2ME2 restores the Crizotinib sensitivity of K562 under hypoxic conditions by inhibiting the activity of HIF1 α [28], which promotes apoptosis possibly mediated by the overexpression of the Bcl2, Bcl-XL and c-myc genes [18].

K562 HIF1 α cells when exposed to 1000 nM Imatinib, Crizotinib, ponatinib, or GNF-5. (C) Proliferation blot of the different K562 cells that were exposed to different concentrations of Crizotinib. Cell viability was monitored as described in Materials and Methods. *p-value ≤ 0.01 , **p-value ≤ 0.001 , * p-value ≤ 0.0001 . The experiment was run in duplicate and repeated (for a total of two independent experimental runs), with both yielding comparable outcomes.**

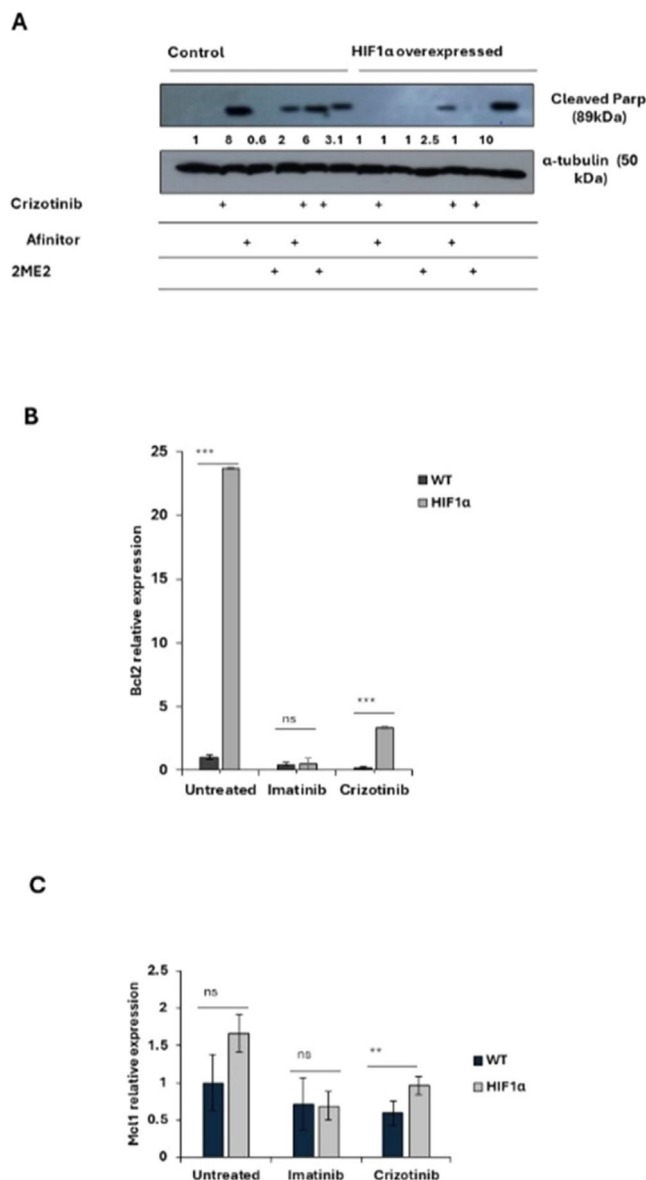


Figure 5 – Effect of 2ME2 on HIF1 α -mediated resistance to Crizotinib. K562 or K562/HIF1 α cells were treated with 1 % DMSO, Imatinib, Crizotinib, Afinitor, or 2ME2 for 24 h. (A) Immunoblot of K562 or K562/HIF1 α cells treated with 1 μ M Crizotinib, Afinitor, or 2ME2. Filters were probed with anti-c-PARP and α -tubulin antibodies. The numbers below the different lanes represent relative values normalized to α -tubulin. (B and C) Relative expressions of (B) Bcl2 and (C) Mcl1 genes compared to the β -actin gene were determined by real-time PCR using K562 and K562/HIF1 α cells treated with 1 % DMSO, Imatinib, or Crizotinib for 24 h. Sequences of the primers used in this study are shown in Table 1. The levels of PCR amplicons were analyzed using a two-sample t-test. The mean relative expression (log2) \pm standard error of the mean is shown. *p-value ≤ 0.01 , **p-value ≤ 0.001 and *** p-value ≤ 0.0001 . The experiment was performed twice, yielding consistent results.

The data of the present study showed that Ruxolitinib, a JAK1/2 inhibitor, can attenuate the effect of hypoxia or HIF1 α overexpression in mediating Crizotinib resistance in CML cells. Previous studies have shown that JAK1/2 inhibitors such as AG490 promote the accumulation of HIF1 α by inhibiting its hydroxylation [48]. Specifically, JAK1/2 is involved in the activation of prolyl hydroxylase domain enzyme activity in HIF1 α , which mediates the hydroxylation of HIF1 α and its subsequent degradation by the proteasome [48]. Therefore, the JAK1/2 inhibitor Ruxolitinib may inhibit the degradation of HIF1 α and contribute to its stabilization [48]. Other studies have shown that inactivation of JAK1 promotes proliferation of endometrial cancer cells by upregulating the HIF1 α signaling pathway [49]. The authors suggested that JAK1 may act as a tumor suppressor [49], and that deletion of JAK1 activates the HIF1 α pathway [49]. Jeong et al. [50] suggested that JAK1 interacts with HIF-1/2 and reduces the expression of HIF-1/2 protein under hypoxia; therefore, silencing of JAK1 or pharmacologic inhibition of JAK1 kinase activity by Ruxolitinib leading to upregulation of transcription of HIF target genes under hypoxia. Crizotinib may affect the stability of HIF1 α in a JAK2-dependent manner, as suggested by the observation that Crizotinib inhibits JAK2 activity [50]. Since Imatinib does not inhibit JAK2, no stabilizing effect is observed in CML cells treated with Imatinib. Furthermore, the activity of Crizotinib was additive to that of Ruxolitinib, which may suggest that different mechanisms are involved in stimulating the stability and function of HIF1 α .

In conclusion, this study shows that hypoxic conditions and the presence of Ruxolitinib contribute to a substantial increase in chemoresistance of CML cells to Crizotinib. Although the ability of Crizotinib to inhibit Bcr/Abl activity remained unchanged, its ability to induce apoptosis in CML cells was diminished. It found that K562 cells overexpressing HIF1 α exhibited higher levels of the anti-apoptotic genes Bcl2 and MCL-1, suggesting a possible mechanism of action. In addition, this study showed that the inclusion of the HIF1 α inhibitor 2ME2 restored the sensitivity of Crizotinib in CML cells. The findings show that HIF1 α enhances chemoresistance of Crizotinib independent of Bcr/Abl kinase activity in CML cells. Consequently, targeting HIF1 α and the components of this pathway may be critical for overcoming chemoresistance and the complete eradication of CML. In addition, targeting the crosstalk between JAK1/2 and HIF1 α has been shown to be a promising strategy for cancer treatment. This intercellular communication could contribute to drug resistance in hypoxic tumor environments. Inhibitors of JAK1/2 or HIF1 α or drugs targeting their downstream signaling pathways have great potential for cancer therapy.

Funding

No external funding for this project.

Ethics approval and consent to participate

Not applicable.

Patient consent for publication

Not applicable.

Data availability

The data that support the findings of this study are available from the corresponding author upon reasonable request.

Conflicts of interest

The authors declare that they have no known competing financial interests or personal relationships that could have appeared to influence the work reported in this paper.

CRediT authorship contribution statement

Lena Avinery: Conceptualization, Investigation, Methodology, Writing – original draft. **Danielle Regev:** Investigation, Methodology, Writing – review & editing. **Hazem Khamaisi:** Conceptualization, Investigation, Methodology. **Jacob Gopas:** Conceptualization, Writing – review & editing, Formal analysis, Resources. **Jamal Mahajna:** Conceptualization, Writing – original draft, Writing – review & editing, Supervision, Formal analysis, Resources.

Acknowledgments

The following plasmids were provided to us by addgene.org. pCMV-VSV-G was a gift from Bob Weinberg (Addgene plasmid # 8454; <http://n2t.net/addgene:8454>; RRID:Addgene_8454). pCMV-dR8.2 dvpr was a gift from Bob Weinberg (Addgene plasmid # 8455; <http://n2t.net/addgene:8455>; RRID: Addgene_8455). LentiCas9 blast was a gift from Feng Zhang (Addgene plasmid # 52962; <http://n2t.net/addgene:52962>; RRID: Addgene_52962). HA-HIF1α P402A/P564A-pBabe-puro was a gift from William Kaelin (Addgene plasmid # 19005; <http://n2t.net/addgene:19005>; RRID: Addgene_19005). JAK2 gRNA (BRDN0001149125) was a gift from John Doench & David Root (Addgene plasmid # 75728; <http://n2t.net/addgene:75728>; RRID: Addgene_75728).

Editor Eduardo Rego.

REFERENCES

- Faderl S, Talpaz M, Estrov Z, O'Brien S, Kurzrock R, Kantarjian HM. The biology of chronic myeloid leukemia. *N Engl J Med*. 1999;341(3):164–72. [Internet]Jul 15 [cited 2024 Nov 3] Available from: <https://pubmed.ncbi.nlm.nih.gov/10403855/>.
- Radich JP, Dai H, Mao M, Oehler V, Schelter J, Druker B, et al. Gene expression changes associated with progression and response in chronic myeloid leukemia. *Proc Natl Acad Sci U S A*. 2006;103(8):2794. [Internet]Feb 21 [cited 2024 Nov 3] Available from: <https://pmc.ncbi.nlm.nih.gov/articles/PMC1413797/>.
- Gambacorti-Passerini CB, Gunby RH, Piazza R, Galiotta A, Rostagno R, Scapozza L. Molecular mechanisms of resistance to imatinib in Philadelphia-chromosome-positive leukaemias. *Lancet Oncol*. 2003;4(2):75–85. Feb 1.
- Katz BZ, Polliack A. Cancer microenvironment, extracellular matrix, and adhesion molecules: the bitter taste of sugars in chronic lymphocytic leukemia. *Leuk Lymphoma*. 2011;52(9):1619–20. [Internet][cited 2024 Nov 3] Available from: <https://www.tandfonline.com/action/journalInformation?journalCode=ilal20>.
- Tesfai Y, Ford J, Carter KW, Firth MJ, O'Leary RA, Gottardo NG, et al. Interactions between acute lymphoblastic leukemia and bone marrow stromal cells influence response to therapy. *Leuk Res*. 2012;36(3):299–306. Mar 1.
- Minakata K, Takahashi F, Nara T, Hashimoto M, Tajima K, Murakami A, et al. Hypoxia induces gefitinib resistance in non-small-cell lung cancer with both mutant and wild-type epidermal growth factor receptors. *Cancer Sci*. 2012;103(11):1946. [Internet]Nov [cited 2024 Nov 3] Available from: <https://pmc.ncbi.nlm.nih.gov/articles/PMC7659171/>.
- Jensen P.E., Mortensen B.T., Hodgkiss R.J., Iversen P.O., Christensen I.J., Helledie N., et al. Increased cellular hypoxia and reduced proliferation of both normal and leukaemic cells during progression of acute myeloid leukaemia in rats. *QJ*.
- Dengler VL, Galbraith MD, Espinosa JM. Transcriptional regulation by hypoxia inducible factors. *Crit Rev Biochem Mol Biol*. 2013;49(1):1. [Internet]Jan [cited 2024 Nov 3] Available from: <https://pmc.ncbi.nlm.nih.gov/articles/PMC4342852/>.
- Murakami A, Takahashi F, Nurwidya F, Kobayashi I, Minakata K, Hashimoto M, et al. Hypoxia increases gefitinib-resistant lung cancer stem cells through the activation of insulin-like growth factor 1 receptor. *PLoS One*. 2014;9(1):e86459. [Internet]Jan 28 [cited 2024 Nov 3] Available from: <https://pmc.ncbi.nlm.nih.gov/articles/PMC3904884/>.
- Traer E, Javidi-Sharifi N, Agarwal A, Dunlap J, English I, Martinez J, et al. Ponatinib overcomes FGF2-mediated resistance in CML patients without kinase domain mutations. *Blood*. 2014;123(10):1516–24. <https://doi.org/10.1182/blood-2013-07-518381>. [Internet]Mar 6 [cited 2024 Nov 3].
- Regev O, Kidan N, Nicola M, Khamisie H, Mahajna J. Crizotinib overcomes microenvironment-mediated drug resistance in ph-positive leukemia. *Cancer Sci Ther*. 2018;10. [Internet] [cited 2024 Nov 4] Available from: <https://www.hilarispublisher.com/proceedings/crizotinib-overcomes-microenvironment-mediated-drug-resistance-in-phpositive-leukemia-32581.html>.
- Ng KP, Manjeri A, Lee KL, Huang W, Tan SY, Chuah CTH, et al. Physiologic hypoxia promotes maintenance of CML stem cells despite effective BCR-ABL1 inhibition. *Blood*. 2014;123(21):3316–26. <https://doi.org/10.1182/blood-2013-07-511907>. [Internet]May 22 [cited 2024 Nov 3].
- Jiang M, He G, Wang J, Guo X, Zhao Z, Gao J, et al. Hypoxia induces inflammatory microenvironment by priming specific macrophage polarization and modifies LSC behaviour via VEGF-HIF1α signalling. *Transl Pediatr*. 2021;10(7). <https://doi.org/10.21037/tp-21-86>. [Internet][cited 2024 Nov 3].
- Kidan N, Khamaisie H, Ruimi N, Roitman S, Eshel E, Dally N, et al. Ectopic expression of snail and twist in ph+ leukemia cells upregulates CD44 expression and alters their differentiation potential. *J Cancer*. 2017;8(19):3952–68. [Internet][cited 2024 Nov 3] Available from: <http://www.jcancer.org>.

15. Yan Q, Bartz S, Mao M, Li L, Kaelin WG. The hypoxia-inducible factor 2 N-terminal and C-terminal transactivation domains cooperate to promote renal tumorigenesis *In vivo*. *Mol Cell Biol*. 2007;27(6):3.
16. Stewart SA, Dykxhoorn DM, Palliser D, Mizuno H, Yu EY, An DS, et al. Lentivirus-delivered stable gene silencing by RNAi in primary cells. *RNA*. 2003;9(4):493.. [Internet]Apr 1 [cited 2024 Nov 5] Available from: <https://pmc.ncbi.nlm.nih.gov/articles/PMC1370415/>.
17. Gochman E, Mahajna J, Shenzer P, Dahan A, Blatt A, Elyakim R, et al. The expression of iNOS and nitrotyrosine in colitis and colon cancer in humans. *Acta Histochem*. 2012;114(8):827–35. Dec 1.
18. Koren Carmi Y, Khamaisi H, Adawi R, Noyman E, Gopas J, Mahajna J. Secreted soluble factors from tumor-activated mesenchymal stromal cells confer platinum chemoresistance to ovarian cancer cells. *Int J Mol Sci*. 2023;24(9):7730.. Vol 24, Page 7730 [Internet]. 2023 Apr 23 [cited 2024 Nov 4] Available from: <https://www.mdpi.com/1422-0067/24/9/7730/html>.
19. Dotan N, Wasser SP, Mahajna J. Inhibition of the androgen receptor activity by Coprinus comatus substances. *Nutr Cancer*. 2011;63(8):1316–27. [Internet]Nov 1 [cited 2024 Nov 4] Available from: <https://www.tandfonline.com/doi/abs/10.1080/01635581.2011.607542>.
20. Sahu A, Prabhash K, Noronha V, Joshi A, Desai S. Crizotinib: a comprehensive review. *South Asian J Cancer*. 2013;2(2):91.. [Internet][cited 2024 Nov 4] Available from: <https://pmc.ncbi.nlm.nih.gov/articles/PMC3876666/>.
21. Regev O, Kidan N, Nicola M, Khamisie H, Ruthardt M, Mahajna J. Mesenchymal soluble factors confer imatinib drug resistance in chronic myelogenous leukemia cells. *Arch Med Sci*. 2021;17(1):266–74. [Internet]Jan 5 [cited 2024 Nov 4] Available from: <https://www.archivesofmedicalscience.com/Mesenchymal-soluble-factors-confer-imatinib-drug-resistance-in-chronic-myelogenous,127894,0,2.html>.
22. Wu D, Yotnda P. Induction and testing of hypoxia in cell culture. *J Vis Exp*. 2011(54):e2899.. [Internet]Aug 12 [cited 2024 Nov 4] Available from: <https://app.jove.com/t/2899/induction-and-testing-of-hypoxia-in-cell-culture>.
23. Selvendiran K, Bratasz A, Kuppasamy ML, Tazi MF, Rivera BK, Kuppasamy P. Hypoxia induces chemoresistance in ovarian cancer cells by activation of signal transducer and activator of transcription 3. *Int J Cancer*. 2009;125(9):2198–204. [Internet]Nov 1 [cited 2024 Nov 4] Available from: <https://onlinelibrary.wiley.com/doi/full/10.1002/ijc.24601>.
24. Ostojic A, Vrhovac R, Verstovsek S. Ruxolitinib: a new JAK1/2 inhibitor that offers promising options for treatment of myelofibrosis. *Future Oncol*. 2011;7(9):1035.. [Internet]Sep [cited 2024 Nov 4] Available from: <https://pmc.ncbi.nlm.nih.gov/articles/PMC5147419/>.
25. Snell CE, Turley H, McIntyre A, Li D, Masiero M, Schofield CJ, et al. Proline-hydroxylated hypoxia-inducible factor 1 α (HIF-1 α) upregulation in Human tumours. *PLoS One*. 2014;9(2):e88955. <https://doi.org/10.1371/journal.pone.0088955>. [Internet]Feb 12..
26. Hon WC, Wilson MI, Harlos K, Claridge TDW, Schofield CJ, Pugh CW, et al. Structural basis for the recognition of hydroxyproline in HIF-1 α by pVHL. *Nature*. 2002;417(6892):975–8. [Internet][cited 2024 Nov 4] Available from: <https://pubmed.ncbi.nlm.nih.gov/12050673/>.
27. Krishnamachary B, Penet MF, Nimmagadda S, Mironchik Y, Raman V, Solaiyappan M, et al. Hypoxia regulates CD44 and its variant isoforms through HIF-1 α in triple negative breast cancer. *PLoS One*. 2012;7(8):e44078. [Internet]Aug 28 [cited 2024 Nov 4] Available from: <https://journals.plos.org/plosone/article?id=10.1371/journal.pone.0044078>.
28. Mabeesh NJ, Escuin D, LaVallee TM, Pribluda VS, Swartz GM, Johnson MS, et al. 2ME2 inhibits tumor growth and angiogenesis by disrupting microtubules and dysregulating HIF. *Cancer Cell*. 2003;3(4):363–75. [Internet][cited 2024 Nov 4] Available from: <https://pubmed.ncbi.nlm.nih.gov/12726862/>.
29. Frolova O, Samudio I, Benito J, Jacamo R, Kornblau SM, Markovic A, et al. Regulation of HIF-1 α signaling and chemoresistance in acute lymphocytic leukemia under hypoxic conditions of the bone marrow microenvironment. *Cancer Biol Ther*. 2012;13(10):858–70. [Internet]Aug [cited 2024 Nov 4] Available from: <https://www.tandfonline.com/doi/abs/10.4161/cbt.20838>.
30. Mian AA, Haberbosch I, Khamaisie H, Agbarya A, Pietsch L, Eshel E, et al. Crizotinib acts as ABL1 inhibitor combining ATP-binding with allosteric inhibition and is active against native BCR-ABL1 and its resistance and compound mutants BCR-ABL1T315I and BCR-ABL1T315I-E255K. *Ann Hematol*. 2021;100(8):2023–9. [Internet]Aug 1 [cited 2024 Nov 4] Available from: <https://link.springer.com/article/10.1007/s00277-020-04357-z>.
31. Albadari N, Deng S, Li W. The transcriptional factors HIF-1 and HIF-2 and their novel inhibitors in cancer therapy. *Expert Opin Drug Discov*. 2019;14(7):667–82. [Internet][cited 2024 Nov 4] Available from: <https://www.tandfonline.com/doi/abs/10.1080/17460441.2019.1613370>.
32. Kogita A, Togashi Y, Hayashi H, Sogabe S, Terashima M, De Velasco MA, et al. Hypoxia induces resistance to ALK inhibitors in the H3122 non-small cell lung cancer cell line with an ALK rearrangement via epithelial-mesenchymal transition. *Int J Oncol*. 2014;45(4):1430.. [Internet][cited 2024 Nov 4] Available from: <https://pmc.ncbi.nlm.nih.gov/articles/PMC4151805/>.
33. Adamski J, Price A, Dive C, Makin G. Hypoxia-induced cytotoxic drug resistance in osteosarcoma is independent of HIF-1 α . *PLoS One*. 2013;8(6). [Internet]Jun 13 [cited 2024 Nov 4] Available from: <https://pubmed.ncbi.nlm.nih.gov/23785417/>.
34. Zhao C, Zhang Q, Yu T, Sun S, Wang W, Liu G. Hypoxia promotes drug resistance in osteosarcoma cells via activating AMP-activated protein kinase (AMPK) signaling. *J Bone Oncol*. 2016;5(1):22–9. Mar 1.
35. Duval K, Grover H, Han LH, Mou Y, Pegoraro AF, Fredberg J, et al. Modeling physiological events in 2D vs. 3D cell culture. *Physiology*. 2017;32(4):266–77. [Internet]Jun 14 [cited 2024 Nov 4] Available from: <https://journals.physiology.org/doi/10.1152/physiol.00036.2016>.
36. Lancaster MA, Knoblich JA. Organogenesis in a dish: modeling development and disease using organoid technologies. *Science* (1979). 2014;345(6194). [Internet]Jul 18 [cited 2024 Nov 4] Available from: <https://www.science.org/doi/10.1126/science.1247125>.
37. Souza AG, Silva IBB, Campos-Fernandez E, Barcelos LS, Souza JB, Marangoni K, et al. Comparative assay of 2D and 3D cell culture models: proliferation, gene expression and anticancer drug response. *Curr Pharm Des*. 2018;24(15):1689–94. [Internet]May 17 [cited 2024 Nov 4] Available from: <https://www.eurekaselect.com/article/89524>.
38. Petit C, Gouel F, Dubus I, Heuclin C, Roget K, Vannier JP. Hypoxia promotes chemoresistance in acute lymphoblastic leukemia cell lines by modulating death signaling pathways. *BMC Cancer*. 2016;16(1):1–17. [Internet]Sep 22 [cited 2024 Nov 4] Available from: <https://bmccancer.biomedcentral.com/articles/10.1186/s12885-016-2776-1>.
39. Joseph JP, Harishankar MK, Pillai AA, Devi A. Hypoxia induced EMT: a review on the mechanism of tumor progression and metastasis in OSCC. *Oral Oncol*. 2018;80:23–32. May 1.
40. Lin H, Jiang X, Zhu H, Jiang W, Dong X, Qiao H, et al. 2ME2 inhibits the activated hypoxia-inducible pathways by cabozantinib and enhances its efficacy against medullary thyroid

- carcinoma. *Tumour Biol.* 2016;37(1):381–91. [Internet]Jan 1
[cited 2024 Nov 4] Available from: <https://pubmed.ncbi.nlm.nih.gov/26219898/>.
41. Azab SS, Salama SA, Hassan MH, Khalifa AE, El-Demerdash E, Fouad H, et al. 2-Methoxyestradiol reverses doxorubicin resistance in human breast tumor xenograft. *Cancer Chemother Pharmacol.* 2008;62(5):893–902. [Internet]Oct [cited 2024 Nov 4] Available from: <https://pubmed.ncbi.nlm.nih.gov/18253735/>.
42. Chauhan D, Catley L, Hideshima T, Li G, Leblanc R, Gupta D, et al. 2-Methoxyestradiol overcomes drug resistance in multiple myeloma cells. *Blood.* 2002;100(6):2187–94. Sep 15.
43. Lakhani NJ, Sarkar MA, Venitz J, Figg WD. 2-Methoxyestradiol, a promising anticancer agent. *Pharmacotherapy.* 2003;23(2):165–72. [Internet]Feb 1 [cited 2024 Nov 4] Available from: <https://pubmed.ncbi.nlm.nih.gov/12587805/>.
44. Khamaisi H, Mahmoud H, Mahajna J. 2-Hydroxyestradiol overcomes mesenchymal stem cells-mediated platinum chemoresistance in ovarian cancer cells in an ERK-independent fashion. *Molecules.* 2022;27(3). [Internet] Feb 1 [cited 2024 Nov 4] Available from: <https://pubmed.ncbi.nlm.nih.gov/35164068/>.
45. Zhang Y, Chen H, Shen Y, Zhou X. Combined effects of 2-methoxyestradiol (Hypoxia-Inducible Factor 1 α Inhibitor) and dasatinib (A Second-Generation Tyrosine Kinase Inhibitor) on chronic myelocytic leukemia cells. *J Immunol Res.* 2022;2022:6324326. [Internet][cited 2024 Nov 4] Available from: <https://pmc.ncbi.nlm.nih.gov/articles/PMC9071866/>.
46. Van Veldhuizen PJ, Ray G, Banerjee S, Dhar G, Kambhampati S, Dhar A, et al. 2-Methoxyestradiol modulates β -catenin in prostate cancer cells: a possible mediator of 2-methoxyestradiol-induced inhibition of cell growth. *Int J Cancer.* 2008;122(3):567–71. [Internet]Feb 1 [cited 2024 Nov 4] Available from: <https://onlinelibrary.wiley.com/doi/full/10.1002/ijc.23117>.
47. LaVallee TM, Zhan XH, Johnson MS, Herbstritt CJ, Swartz G, Williams MS, et al. 2-Methoxyestradiol up-regulates death receptor 5 and induces apoptosis through activation of the extrinsic pathway. *Cancer Res.* 2003;63(2):468–75. Jan 15.
48. Hernandez-Luna MA, Rocha-Zavaleta L, Vega MI, Huerta-Yepez S. Hypoxia inducible factor-1 α induces chemoresistance phenotype in non-hodgkin lymphoma cell line via up-regulation of bcl-xL. *Leuk Lymphoma.* 2013;54(5):1048–55.
49. Fernandez-Sanchez R, Berzal S, Sanchez-Nino MD, Neria F, Goncalves S, Calabia O, et al. AG490 promotes HIF-1 α accumulation by inhibiting its hydroxylation. *Curr Med Chem.* 2012;19(23):4014–23. [Internet]Jul 25 [cited 2024 Nov 4] Available from: <https://pubmed.ncbi.nlm.nih.gov/22709000/>.
50. Jeong CH, Lee HJ, Cha JH, Jeong HK, Kwang RK, Kim JH, et al. Hypoxia-inducible factor-1 α inhibits self-renewal of mouse embryonic stem cells in Vitro via negative regulation of the leukemia inhibitory factor-STAT3 pathway. *J Biol Chem.* 2007;282(18):13672–9. [Internet]Mar 14 [cited 2024 Nov 4] Available from: <https://europepmc.org/article/med/17360716>.